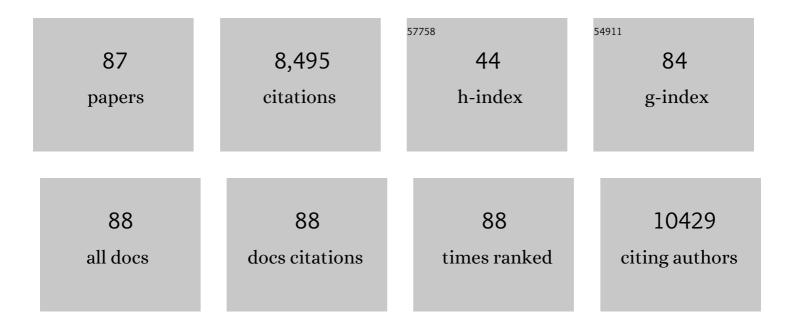
## Chunming Niu

List of Publications by Year in descending order

Source: https://exaly.com/author-pdf/1054599/publications.pdf Version: 2024-02-01



#	Article	IF	CITATIONS
1	Porous Co2VO4 Nanodisk as a High-Energy and Fast-Charging Anode for Lithium-Ion Batteries. Nano-Micro Letters, 2022, 14, 5.	27.0	93
2	Ni3Si2@TiO2 furs for supercapacitors with extremely high areal density and high cycleability. Journal of Alloys and Compounds, 2021, 858, 157711.	5.5	4
3	Synthesis and luminescence studies of mixed phase LiCa3MgV3-XWXO12 phosphors for enhanced quantum yield. Journal of Luminescence, 2021, 234, 117948.	3.1	7
4	PEDOT-Coated Red Phosphorus Nanosphere Anodes for Pseudocapacitive Potassium-Ion Storage. Nanomaterials, 2021, 11, 1732.	4.1	5
5	Inâ€doped LiCa <sub>2.98</sub> MgV <sub>3</sub> O <sub>12</sub> rareâ€earthâ€free phosphor with a high photoluminescence quantum yield of 67.4%. Journal of the American Ceramic Society, 2021, 104, 5837-5847.	3.8	3
6	Core–Shell Co <sub>2</sub> VO <sub>4</sub> /Carbon Composite Anode for Highly Stable and Fast-Charging Sodium-Ion Batteries. ACS Applied Materials & Interfaces, 2021, 13, 55020-55028.	8.0	65
7	Silicon carbide nanowire covered by vertically oriented graphene for enhanced electromagnetic wave absorption performance. Chemical Physics, 2020, 529, 110574.	1.9	21
8	Core-shell structured carbon nanotubes/N-doped carbon layer nanocomposites for supercapacitor electrodes. Journal of Nanoparticle Research, 2020, 22, 1.	1.9	14
9	Ultrathin dense double-walled carbon nanotube membrane for enhanced lithium-sulfur batteries. Journal of Nanoparticle Research, 2020, 22, 1.	1.9	5
10	Comprehensive understanding the promoting effect of Dy-doping on MnFeOx nanowires for the low-temperature NH3-SCR of NOx: An experimental and theoretical study. Journal of Catalysis, 2019, 380, 55-67.	6.2	85
11	Constructing hollow silkworm structure in MnOx–TiO2 catalysts for improving the performance in selective catalytic reduction of NO by NH3. Reaction Kinetics, Mechanisms and Catalysis, 2019, 128, 681-693.	1.7	5
12	Chemical vapor deposition growth of carbon nanotube confined nickel sulfides from porous electrospun carbon nanofibers and their superior lithium storage properties. Nanoscale Advances, 2019, 1, 656-663.	4.6	17
13	The synergistic effects between Ce and Cu in Cu <sub>y</sub> Ce <sub>1â°y</sub> W <sub>5</sub> O <sub>x</sub> catalysts for enhanced NH <sub>3</sub> -SCR of NO <sub>x</sub> and SO <sub>2</sub> tolerance. Catalysis Science and Technology, 2019, 9, 718-730.	4.1	47
14	Classification of MAOX phases and semiconductor screening for next-generation energy conversion ceramic materials. Journal of Materials Chemistry C, 2019, 7, 6895-6899.	5.5	1
15	Two-dimensional eclipsed arrangement hybrid perovskites for tunable energy level alignments and photovoltaics. Journal of Materials Chemistry C, 2019, 7, 5139-5147.	5.5	22
16	Rock-salt and helix structures of silver iodides under ambient conditions. National Science Review, 2019, 6, 767-774.	9.5	11
17	Ligninâ€Derived Holey, Layered, and Thermally Conductive 3D Scaffold for Lithium Dendrite Suppression. Small Methods, 2019, 3, 1800539.	8.6	39
18	Construction of three-dimensional ordered porous carbon bulk networks for high performance lithium-sulfur batteries. Journal of Colloid and Interface Science, 2019, 533, 445-451.	9.4	25

#	Article	IF	CITATIONS
19	Charge-redistribution-induced new active sites on (0â€ <sup>-</sup> 0â€ <sup>-</sup> 1) facets of α-Mn2O3 for significantly enhanced selective catalytic reduction of NO by NH3. Journal of Catalysis, 2019, 370, 30-37.	6.2	54
20	A Facile Path to Grapheneâ€Wrapped Polydopamineâ€Entwined Silicon Nanoparticles with High Electrochemical Performance. ChemPlusChem, 2019, 84, 203-209.	2.8	9
21	The lithium and sodium storage performances of phosphorus and its hierarchical structure. Nano Research, 2019, 12, 1-17.	10.4	63
22	Au Nanoparticle and CdS Quantum Dot Codecoration of In <sub>2</sub> O <sub>3</sub> Nanosheets for Improved H <sub>2</sub> Evolution Resulting from Efficient Light Harvesting and Charge Transfer. ACS Sustainable Chemistry and Engineering, 2019, 7, 547-557.	6.7	44
23	Au decorated hollow ZnO@ZnS heterostructure for enhanced photocatalytic hydrogen evolution: The insight into the roles of hollow channel and Au nanoparticles. Applied Catalysis B: Environmental, 2019, 244, 748-757.	20.2	144
24	Template synthesis of graphitic hollow carbon nanoballs as supports for SnO <sub>x</sub> nanoparticles towards enhanced lithium storage performance. Nanoscale, 2018, 10, 6159-6167.	5.6	50
25	Encapsulating Silica/Antimony into Porous Electrospun Carbon Nanofibers with Robust Structure Stability for High-Efficiency Lithium Storage. ACS Nano, 2018, 12, 3406-3416.	14.6	149
26	Stable 1T-phase MoS <sub>2</sub> as an effective electron mediator promoting photocatalytic hydrogen production. Nanoscale, 2018, 10, 9292-9303.	5.6	60
27	Direct growth of 3D host on Cu foil for stable lithium metal anode. Energy Storage Materials, 2018, 13, 323-328.	18.0	92
28	WS <sub>2</sub> /Graphitic Carbon Nitride Heterojunction Nanosheets Decorated with CdS Quantum Dots for Photocatalytic Hydrogen Production. ChemSusChem, 2018, 11, 1187-1197.	6.8	129
29	Pyrolytic synthesis of MoO3 nanoplates within foam-like carbon nanoflakes for enhanced lithium ion storage. Journal of Colloid and Interface Science, 2018, 514, 686-693.	9.4	24
30	NiyCo1-yMn2Ox microspheres for the selective catalytic reduction of NOx with NH3: The synergetic effects between Ni and Co for improving low-temperature catalytic performance. Applied Catalysis A: General, 2018, 560, 1-11.	4.3	29
31	Multiple carrier-transfer pathways in a flower-like In <sub>2</sub> S <sub>3</sub> /CdIn <sub>2</sub> S <sub>4</sub> /In <sub>2</sub> O <sub>3</sub> ternary heterostructure for enhanced photocatalytic hydrogen production. Nanoscale, 2018, 10, 7860-7870.	5.6	98
32	First-principles insights into tin-based two-dimensional hybrid halide perovskites for photovoltaics. Journal of Materials Chemistry A, 2018, 6, 5652-5660.	10.3	71
33	Preparation and Characterization of Epoxy and Hollow Ceramic Spheres Composites. , 2018, , .		Ο
34	Preparation and Characterization of Epoxy and Hollow Ceramic Spheres Composites. , 2018, , .		0
35	Gd-modified MnOx for the selective catalytic reduction of NO by NH3: The promoting effect of Gd on the catalytic performance and sulfur resistance. Chemical Engineering Journal, 2018, 348, 820-830.	12.7	170
36	Efficient spatial charge separation and transfer in ultrathin g-C <sub>3</sub> N <sub>4</sub> nanosheets modified with Cu <sub>2</sub> MoS <sub>4</sub> as a noble metal-free co-catalyst for superior visible light-driven photocatalytic water splitting. Catalysis Science and Technology, 2018, 8, 3883-3893.	4.1	42

#	Article	IF	CITATIONS
37	Mnâ^'Co Mixed Oxide Nanosheets Vertically Anchored on H <sub>2</sub> Ti <sub>3</sub> O <sub>7</sub> Nanowires: Full Exposure of Active Components Results in Significantly Enhanced Catalytic Performance. ChemCatChem, 2018, 10, 2833-2844.	3.7	39
38	TiC MXene High Energy Density Cathode for Lithium–Air Battery. Advanced Theory and Simulations, 2018, 1, 1800059.	2.8	21
39	Sulfur and Water Resistance of Mn-Based Catalysts for Low-Temperature Selective Catalytic Reduction of NOx: A Review. Catalysts, 2018, 8, 11.	3.5	94
40	"Fast SCR" reaction over Sm-modified MnOx-TiO2 for promoting reduction of NOx with NH3. Applied Catalysis A: General, 2018, 564, 102-112.	4.3	130
41	Layered Hexagonal Oxycarbides, Mn+1AO2Xn (M = Sc, Y, La, Cr, and Mo; A = Ca; X = C): Unexpected Photovoltaic Ceramics. Journal of Physical Chemistry C, 2018, 122, 14240-14247.	3.1	3
42	Enhanced cycling stability of ring-shaped phosphorus inside multi-walled carbon nanotubes as anodes for lithium-ion batteries. Journal of Materials Chemistry A, 2018, 6, 2540-2548.	10.3	39
43	Assembly of Ringâ€ <del>S</del> haped Phosphorus within Carbon Nanotube Nanoreactors. Angewandte Chemie, 2017, 129, 1876-1880.	2.0	21
44	Assembly of Ringâ€ <b>S</b> haped Phosphorus within Carbon Nanotube Nanoreactors. Angewandte Chemie - International Edition, 2017, 56, 1850-1854.	13.8	64
45	Honeycomb-like carbon nanoflakes as a host for SnO <sub>2</sub> nanoparticles allowing enhanced lithium storage performance. Journal of Materials Chemistry A, 2017, 5, 6817-6824.	10.3	101
46	MnM2O4 microspheres (M = Co, Cu, Ni) for selective catalytic reduction of NO with NH3: Comparative study on catalytic activity and reaction mechanism via in-situ diffuse reflectance infrared Fourier transform spectroscopy. Chemical Engineering Journal, 2017, 325, 91-100.	12.7	95
47	Rationally Designed Porous MnO <sub><i>x</i></sub> –FeO <sub><i>x</i></sub> Nanoneedles for Low-Temperature Selective Catalytic Reduction of NO <sub><i>x</i></sub> by NH <sub>3</sub> . ACS Applied Materials & Interfaces, 2017, 9, 16117-16127.	8.0	164
48	Bird's nest-like nanographene shell encapsulated Si nanoparticles – Their structural and Li anode properties. Journal of Power Sources, 2017, 341, 46-52.	7.8	32
49	Fabrication of g <sub>3</sub> N <sub>4</sub> /Au/Câ€TiO <sub>2</sub> Hollow Structures as Visibleâ€Lightâ€Driven Zâ€6cheme Photocatalysts with Enhanced Photocatalytic H <sub>2</sub> Evolution. ChemCatChem, 2017, 9, 3752-3761.	3.7	114
50	Porous MnOx for low-temperature NH3-SCR of NOx: the intrinsic relationship between surface physicochemical property and catalytic activity. Journal of Nanoparticle Research, 2017, 19, 1.	1.9	15
51	A Hierarchical Phosphorus Nanobarbed Nanowire Hybrid: Its Structure and Electrochemical Properties. Nano Letters, 2017, 17, 3376-3382.	9.1	39
52	Binding SnO2 nanoparticles onto carbon nanotubes with assistance of amorphous MoO3 towards enhanced lithium storage performance. Journal of Colloid and Interface Science, 2017, 504, 230-237.	9.4	22
53	Mn/CeO 2 catalysts for SCR of NO x with NH 3 : comparative study on the effect of supports on low-temperature catalytic activity. Applied Surface Science, 2017, 411, 338-346.	6.1	142
54	Pseudo-topotactic conversion of carbon nanotubes to T-carbon nanowires under picosecond laser irradiation in methanol. Nature Communications, 2017, 8, 683.	12.8	184

#	Article	IF	CITATIONS
55	Epitaxial Growth of Urchinâ€Like CoSe <sub>2</sub> Nanorods from Electrospun Coâ€Embedded Porous Carbon Nanofibers and Their Superior Lithium Storage Properties. Particle and Particle Systems Characterization, 2017, 34, 1700185.	2.3	49
56	Eu-Mn-Ti mixed oxides for the SCR of NOx with NH3: The effects of Eu-modification on catalytic performance and mechanism. Fuel Processing Technology, 2017, 167, 322-333.	7.2	64
57	MnO x -TiO 2 and Sn doped MnO x -TiO 2 selective reduction catalysts prepared using MWCNTs as the pore template. Chemical Engineering Journal, 2017, 327, 1-8.	12.7	28
58	Highly Efficient Photocatalyst Based on a CdS Quantum Dots/ZnO Nanosheets 0D/2D Heterojunction for Hydrogen Evolution from Water Splitting. ACS Applied Materials & Interfaces, 2017, 9, 25377-25386.	8.0	235
59	Rational design of CdS@ZnO core-shell structure via atomic layer deposition for drastically enhanced photocatalytic H2 evolution with excellent photostability. Nano Energy, 2017, 39, 183-191.	16.0	195
60	Highly Crystallized C-Doped Mesoporous Anatase TiO2 with Visible Light Photocatalytic Activity. Catalysts, 2016, 6, 117.	3.5	39
61	Synthesis of Hierarchical Sb <sub>2</sub> MoO <sub>6</sub> Architectures and Their Electrochemical Behaviors as Anode Materials for Li-Ion Batteries. Inorganic Chemistry, 2016, 55, 7012-7019.	4.0	35
62	Manganese oxide-based catalysts for low-temperature selective catalytic reduction of NO x with NH 3 : A review. Applied Catalysis A: General, 2016, 522, 54-69.	4.3	394
63	Ni3Si2 nanowires grown in situ on Ni foam for high-performance supercapacitors. Journal of Power Sources, 2016, 320, 13-19.	7.8	44
64	C-doped mesoporous anatase TiO 2 comprising 10 nm crystallites. Journal of Colloid and Interface Science, 2016, 476, 1-8.	9.4	42
65	Interfacial engineering of Si/multi-walled carbon nanotube nanocomposites towards enhanced lithium storage performance. Carbon, 2016, 107, 600-606.	10.3	36
66	Hydrothermal Synthesis of SnO2 Embedded MoO3-x Nanocomposites and Their Synergistic Effects on Lithium Storage. Electrochimica Acta, 2016, 216, 79-87.	5.2	48
67	Nanocarved MoS <sub>2</sub> –MoO <sub>2</sub> Hybrids Fabricated Using <i>in Situ</i> Grown MoS <sub>2</sub> as Nanomasks. ACS Nano, 2016, 10, 9509-9515.	14.6	52
68	MnOx-CeO2 shell-in-shell microspheres for NH3-SCR de-NOx at low temperature. Catalysis Communications, 2016, 86, 36-40.	3.3	61
69	Synthesis of SnO <sub>2</sub> versus Sn crystals within N-doped porous carbon nanofibers via electrospinning towards high-performance lithium ion batteries. Nanoscale, 2016, 8, 7595-7603.	5.6	69
70	Highly Efficient Flexible Perovskite Solar Cells Using Solution-Derived NiO <sub><i>x</i></sub> Hole Contacts. ACS Nano, 2016, 10, 3630-3636.	14.6	426
71	Energy Storage: Ternary Sn-Ti-O Based Nanostructures as Anodes for Lithium Ion Batteries (Small) Tj ETQq1 1 (	0.784314 rg 10.0	BT /Overlock
72	CdS quantum dots modified N-doped titania plates for the photocatalytic mineralization of diclofenac	4.8	27

in water under visible light irradiation. Journal of Molecular Catalysis A, 2015, 399, 79-85.

#	Article	IF	CITATIONS
73	Preparation of nanographite sheets supported Si nanoparticles by in situ reduction of fumed SiO 2 with magnesium for lithium ion battery. Journal of Power Sources, 2015, 281, 425-431.	7.8	57
74	Carbon-doped titania nanoplates with exposed {001} facets: facile synthesis, characterization and visible-light photocatalytic performance. RSC Advances, 2015, 5, 17667-17675.	3.6	16
75	Carbon nanotube hybrids with MoS2 and WS2 synthesized with control of crystal structure and morphology. Carbon, 2015, 85, 168-175.	10.3	38
76	In Situ Synthesis of Carbon Nanotube Hybrids with Alternate MoC and MoS <sub>2</sub> to Enhance the Electrochemical Activities of MoS <sub>2</sub> . Nano Letters, 2015, 15, 5268-5272.	9.1	84
77	SnO <sub>2</sub> nanoarrays for energy storage and conversion. CrystEngComm, 2015, 17, 5593-5604.	2.6	27
78	Adsorption and Deposition of Li <sub>2</sub> O <sub>2</sub> on the Pristine and Oxidized TiC Surface by First-principles Calculation. Journal of Physical Chemistry C, 2015, 119, 25684-25695.	3.1	32
79	Growth of Ultrafine SnO 2 Nanoparticles within Multiwall Carbon Nanotube Networks: Non-Solution Synthesis and Excellent Electrochemical Properties as Anodes for Lithium Ion Batteries. Electrochimica Acta, 2015, 178, 778-785.	5.2	52
80	Defect chemistry and lithium transport in Li <sub>3</sub> OCl anti-perovskite superionic conductors. Physical Chemistry Chemical Physics, 2015, 17, 32547-32555.	2.8	105
81	Carbon-doped titania flakes with an octahedral bipyramid skeleton structure for the visible-light photocatalytic mineralization of ciprofloxacin. RSC Advances, 2015, 5, 98361-98365.	3.6	14
82	Ternary Sn–Ti–O Based Nanostructures as Anodes for Lithium Ion Batteries. Small, 2015, 11, 1364-1383.	10.0	47
83	Adsorption and Deposition of Li <sub>2</sub> O <sub>2</sub> on TiC{111} Surface. Journal of Physical Chemistry Letters, 2014, 5, 3919-3923.	4.6	30
84	Carbon nanotube transparent conducting films. MRS Bulletin, 2011, 36, 766-773.	3.5	60
85	High-performance thin-film transistors using semiconductor nanowires and nanoribbons. Nature, 2003, 425, 274-278.	27.8	895
86	High power electrochemical capacitors based on carbon nanotube electrodes. Applied Physics Letters, 1997, 70, 1480-1482.	3.3	1,300
87	Experimental Realization of the Covalent Solid Carbon Nitride. Science, 1993, 261, 334-337.	12.6	878